

Spatial patterns of visual cortical fast EEG during conditioned reflex in a rhesus monkey

Walter J. Freeman¹ and Bob W. van Dijk²

¹Department of Physiology–Anatomy, University of California, Berkeley CA 94720 (U.S.A.) and ²The Netherlands Ophthalmic Research Institute, Academic Medical Center, Amsterdam (The Netherlands)

(Accepted 3 March 1987)

Key words: Cortex (visual); EEG (spatial pattern); Monkey (rhesus); Perception (visual); Spatial analysis (EEG); Visual cortex (EEG)

A preliminary assay was made of the existence of time–space coherence patterns of fast EEG activity in the visual cortex of a Rhesus monkey. The primary intent of the present study was to evaluate the similarities and differences in relation to the olfactory bulb, where such coherences have been described and have been demonstrated to be associated with behaviour. Segments 1.5 s in duration were recorded simultaneously without averaging from 16 of 35 subdural electrodes fixed over the left occipital lobe in an array 3.6 cm × 2.8 cm. Each segment was taken during the delivery of a visual conditioned stimulus (CS) and the performance of a conditioned response (CR) by a well-trained Rhesus monkey. The EEGs appeared chaotic with irregular bursts lasting 75–200 ms, resembling those in the olfactory EEG but with lower peak frequencies. Fourier spectra showed broad distributions of power resembling '1/f noise' with multiple peaks in the range of 20–40 Hz. Time intervals were selected where coherent activity seemed to be present at a number of electrodes. A dominant component waveform that was common to all channels was extracted by principal components analysis (PCA) of each segment. The distribution of the power of this component across the electrodes (the factor loadings) was used to describe the spatial pattern of the coherent cortical activity. Statistical analyses suggested that different patterns could be associated to the CS and the CR, as has been found in the olfactory system. These patterns remained stable over a 6 week recording interval. The patterns can be better discriminated, when the factor loadings of each channel are normalized to zero mean and unit variance, to discard a basic pattern of power distribution, which may reflect anatomical and electrode positioning factors that are related to behavioral information processing by the cortex. The wide spatial distribution of the common patterns found suggests that EEG patterns that manifest differing states of the visual cortex may also be accessible with scalp electrodes.

INTRODUCTION

Studies of the EEG of the olfactory bulb and cortex have shown that odor-specific information is manifested in the high frequency range (55–75 Hz in the rabbit, 35–55 Hz in the cat). This information appears to be broadly distributed and to be spatially uniform in density though not in content. Also it has been shown that patterns of coherent variance are associated with different behavioral states⁵. A theory of dynamic function of the olfactory bulb and cortex has been developed to explain olfactory perception^{3–5}. The aim of the present study was to determine whether a similar set of observations and theory might hold for visual cortex, and, if so, to evaluate the experimental conditions that would have to be

dealt with in extracting proof.

The opportunity presented itself in a rhesus monkey already trained to respond to visual cues and having already an array of subdural electrodes surgically fixed onto the occipital lobe². This report describes the preliminary findings and gives some of the conditions that should be met in making effective use of visual cortical EEGs for experimentally testing the validity of non-linear dynamic models of visual information processing similar to those described for the olfactory bulb.

MATERIALS AND METHODS

The adult rhesus monkey ('Chico') had been trained under thirst² to fixate on a square (3' × 3' arc

Correspondence: B.W. van Dijk, The Netherlands Ophthalmic Research Institute, Academic Medical Center, P.O. Box 12141, 1100 AC Amsterdam, The Netherlands.

at 1.72 m) containing a checkerboard pattern (2×2 squares) that flickered at a 7.8 Hz reversal rate and with 20% contrast. The training pattern had a mean retinal illuminance of 96 cd/m^2 ; the surrounding monitor screen had a retinal illuminance of 80 cd/m^2 . The onset of flicker indicated that a trial was beginning; after a time interval randomly varied between 1.5 and 5.0 s, the cessation of the flicker indicated that a pull on a lever between 400 and 600 ms (on some trials 300–500 ms) later would be rewarded by delivery of apple juice. Trials were repeated every 4–6 s while a larger checkerboard in the right upper or lower visual field was shown repeatedly at approximately 1/s (on 340 ms, off 500 ms) without reward contingency. The majority of trials each day were devoted to collecting visual evoked potentials averaged in respect to the reversals of the larger checkerboard.

On each of 8 sessions at approximately weekly intervals a set of 6 trials was used to record monopolarly (with respect to a frontal reference screw) unaveraged EEG time series from 16 independent channels starting at the cessation of the flicker of the training pattern and lasting 1.5 s. Analog filters were set at 0.3 Hz and 105 Hz; the gain was 10K, and the digitizing interval was 4.15 ms. Off-line the data were filtered digitally with a rectangular high-pass filter at 20 Hz and with a notch filter at $50 \text{ Hz} \pm 0.8 \text{ Hz}$ in width to remove interference. The 16 EEG traces were displayed in time segments up to 1508 ms (359 points) in length. Trials with movement or eyeblink artefacts were discarded. Power spectra were computed for selected channels.

A set of 35 subdural electrodes had been implanted over the left visual cortex in the form of 5 bundles 0.6–0.7 cm apart, each having 7 stainless steel wires with exposed tips at intervals of 0.6–0.65 cm. The locations were checked by X-ray with respect to the skull and by visual evoked potentials with respect to the retinal projection onto the cortex². Recordings were from 16 electrodes, either in a contiguous subset in a window $2.4 \times 1.4 \text{ cm}$ over the primary visual cortex covering approximately a lower right quarter circular region with a diameter of 4.5° in the visual field or in an outside subset constituting a window $3.6 \times 2.8 \text{ cm}$ both anterior and posterior to the lunate sulcus and recording activity from Brodmann areas 17, 18 and 19.

The EEG traces were divided into 4 different epochs. Each of these epochs was assumed to be associated with a different behavioral state:

(1) In the first 100 ms after cessation of flicker the EEG associated with the flicker was found. The monkey was fixating and accommodating to the training if he was attentive. The averaged VEP to the cessation of flicker had a latency appreciably longer than 100 ms.

(2) The period from 200 to 400 ms after cessation was associated with the CS onset. The VEP to the cessation had its peaks before this interval.

(3) The period from 400 to 600 ms after the cessation was associated with the CR. The monkey had to push the handlebar to obtain his apple juice reward and invariably looked at the mouthpiece.

(4) The period from 600 to 800 ms after cessation was associated with the UCS. In this period the apple juice reward was given if the monkey responded correctly.

Within each of these epochs shorter time segments were selected by eye in which the EEG appeared to show bursts or coherency across channels. On average these intervals had a duration of 120 ms. In these segments the amount of power that could be attributed to a common waveform was calculated, as well as the distribution of this power across the channels (we will call the amplitude of the common component in each channel the factor loading). The set of factor loadings is treated as an expression of the spatial amplitude distribution of the coherent fast EEG. These spatial patterns will be represented by contour plots of the factor loadings. In practice the time segments were subjected to a principal components analysis (PCA). The PCA was performed using singular value decomposition as described elsewhere⁷. It results in a set of principal components (PCs) and their factor loadings. The dominant PC suffices to characterize the EEG spatial pattern (across channels); it is the only component reported in this study.

To test whether specific spatial patterns of the fast EEG exist associated with CS and CR in visual cortex, we compared the spatial patterns found in the different epochs as well as the patterns found when the monkey responded in a different manner to the CS.

The sets of data were grouped according to whether (1) a correct CR occurred, (2) the CR occurred

outside the correct time frame, or the monkey appeared to be correctly fixating but failed to respond, or (3) the monkey appeared not to be paying attention to the CS.

Quantitative comparisons of the spatial patterns were made in two ways:

(1) By cross-correlating the factor loadings patterns and pooling the values by use of Fisher's Z -transform.

(2) By use of a Euclidean distance measure^{3,5}. In this procedure the average factor loadings pattern was calculated for groups of bursts from each of the 4 epochs (forming 4 different 'centroids'). It was then tested whether an individual pattern was closer to the centroid from its own epoch or to the centroid from another. A Euclidian measure of distance (i.e. the root mean of squared differences of the 16 factor loadings from the mean factor loading) was used. If indeed a burst pattern was closer to its own centroid the classification was 'correct'. This classification was repeated for all burst patterns in the two groups which are compared, the result being a percentage of correctly classified patterns. The deviation of this percentage from 50% describes how different the patterns from the two groups were. To test the significance of the observed differences the test was designed to be used on 2 pairs of centroids. One pair T_1 and T_2 was postulated to differ, a second pair C_1 and C_2 to be equal. The differences between T_1 and T_2 were then corrected for intrinsic bias (e.g. by the segment selection procedure) using the difference between the control centroids. Assuming that the probability to classify the test bursts correctly (P_t) and the probability from intrinsic bias (P_c) were additive one could correct the test result (\bar{P}_t) by subtracting P_c from the proportion of test bursts classified correct \bar{P}_t to obtain an estimate of P_t . Alternatively if P_t and P_c described independent processes correction of the test result could be achieved by

$$P_t = 1 - (1 - \bar{P}_t) / (1 - P_c)^*$$

The value of P_t multiplied by 100 was used to describe the difference between T_1 and T_2 bursts. For olfactory EEGs a significance level of $P = 0.01$ was

associated with a % difference value of 10% or larger³. We assumed similar significance levels in visual cortical fast EEGs. As argued in the results section the spatial patterns of the fast EEG were all strongly similar and also similar to the distribution pattern of the factor loadings of the dominant component in the (averaged) visual evoked potential to the cessation of the training stimulus. This partly reflects the dominance of the foveal projection to the visual cortex and partly differences in anatomic structure or the positioning of the electrodes. For instance, some of the electrodes may have been positioned closer to the cortical sources than others due to sulci or twists in the electrode bundles. For these reasons we have made quantitative comparisons both using the actual variances recorded and using the data after 'channel normalization' to zero mean and unit standard deviation.

RESULTS

The greater part of the power in the EEG was concentrated in the lower end of the spectrum. When this was removed by high-pass filtering, thereby allowing increase in the gain for display, the complex space-time structure of the fast EEG emerged (Fig. 1). Despite its overall chaotic appearance there seemed to be widespread spatial coherence, especially during episodes called 'bursts' lasting 75–200 ms of relatively high amplitude oscillations. This basic structural coherence was clearly not due to a contribution from the reference electrode in monopolar recording, because the amplitude differed between channels. Superimposed on this widespread component were localized and transitory episodes of coherent activity at differing main frequencies, typically located at clustered electrodes near the edges of the 'window' formed by the electrode array (e.g. along the upper or lower bundle in the small window). The EEG traces from the larger window (3.6×2.8 cm) (Fig. 2) gave an impression of more subsidiary activity than in traces from the smaller window especially, at frequencies exceeding 40 Hz and toward the anterior front of the array.

Power spectral analysis of the time segments cho-

* If P_t and P_c are independent the test is classified incorrect only when T_1 and T_2 are not different *and* no bias has occurred, i.e. $1 - P_t = (1 - P_t)(1 - P_c)$.

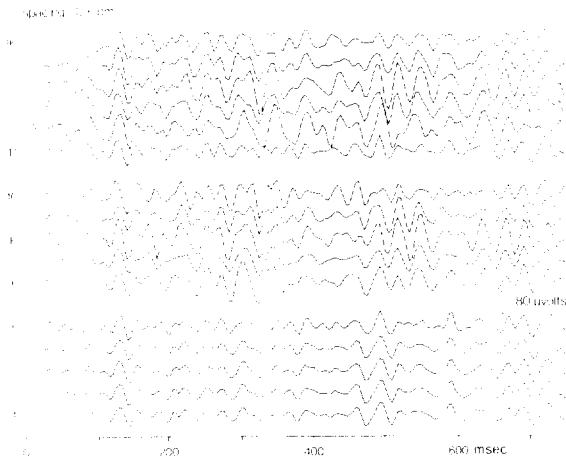


Fig. 1. Sixteen traces simultaneously recorded for a period of 0.75 s from electrodes at spacings of 0.6 cm (3 groups of 5, 5, and 6) along 3 bundles 0.7 cm apart, forming a 2.4×1.4 cm window centered on the foveal cortex at trace 8.

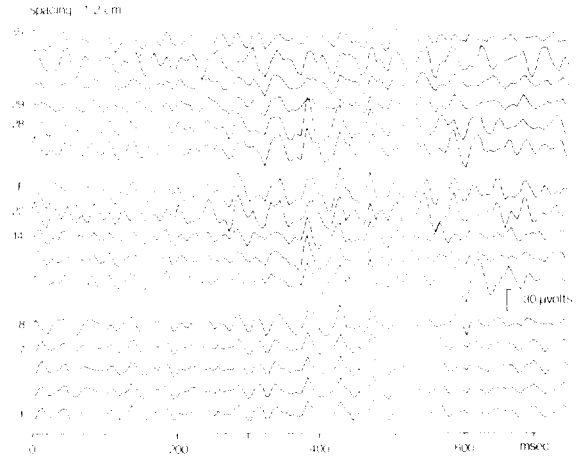


Fig. 2. Sixteen traces at spacings of 1.2–1.4 cm (3.6×2.8 cm window). The spatial commonality by visual inspection appeared to be higher over the smaller window, but PCA and the values for the ratio of temporal and spatial standard deviations did not confirm this apparent difference.

sen (0.754–1.508 s in duration) showed that the energy was broadly distributed over the entire spectrum from 0.3 Hz to 105 Hz (the pass band for recording), it decreased with increasing frequency in the form of '1/f noise' (Fig. 3). On the average the natural log-

arithm of the power decreased by roughly 1/e for each 10 Hz increase. High-pass filtering was arbitrarily chosen with a cut off frequency at 20 Hz to yield the fast EEGs. Transitory spectral peaks appeared at

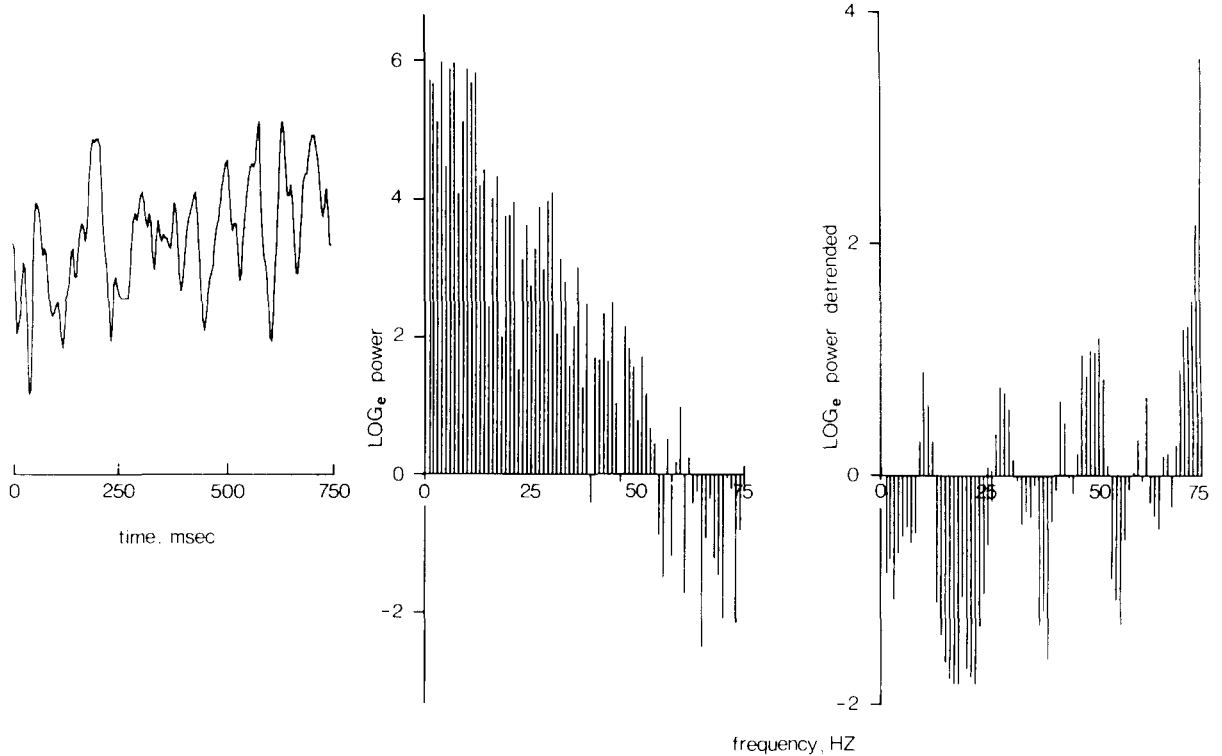


Fig. 3. Left: spatial ensemble average time series. Center: natural logarithm of the power spectrum. Right: spectrum after subtraction of the 1/f trend line computed over the range of 1–75 Hz.

multiple higher frequencies that varied over trials. The spectra of the selected short segments (averaging 120 ms) showed concentration of power into a single peak or at most two peaks in the above range. One dominant peak occurred between 20 and 40 Hz (mean 30.06 ± 3.72 Hz) over a set of 48 spectra. However, when they were averaged, the power spectra of bursts and also of interburst segments revealed the same form resembling '1/f noise'.

No significant differences in overall EEG amplitudes or in spectra were found between sessions, between the 4 time periods sampled within trials, or between the 3 behavioral groups, except that the amplitude of the fast EEG often fell to low levels on trials in which Chico appeared to be inattentive. Instances of equivalently low amplitude (less than 2/3 of the average) were found also in correct trials. The low level of fast EEG tended to be obscured by persisting EEG activity at usual amplitudes in the low spectral range of records prior to high-pass filtering at 20 Hz. No significant spatial pattern differences were found either on changing the presentation of the large checkerboard pattern (not rewarded or punished) from the upper to the lower right quadrant of the visual field or the reverse.

A waveform common to all channels within a burst period could be extracted that incorporated on the average 66.5% of the total variance (range: 52.1–92.3%). Although the spectral distribution of power within samples of this component appeared less wide than that across the 1.5 s time series, its waveforms were more chaotic than sinusoidal. There was no smaller concentration of power into the first component in EEGs from the larger window than from the smaller window.

Contour plots of the factor loadings showed several local maxima and minima of amplitude that closely expressed the variance of the EEG segments. Most often a maximum factor loading was found at an electrode near the cortical site of the foveal projection (Fig. 4). This was also the site of highest amplitude of the averaged evoked potential to the off-set of the fixation target flicker. An ensemble average of the pattern of the dominant component factor loadings

was computed for the 16 channels of the set of bursts from each session. These patterns were cross-correlated with the pattern of the factor loadings of the dominant component of the averaged evoked potential 100–200 ms after the cessation of flicker. The average value by Z-transform over sessions was 0.47 (range: 0.33–1.14). The values for the correlation did not show a trend across sessions, thereby reflecting the stability of the spatial pattern of the EEG amplitude across sessions.

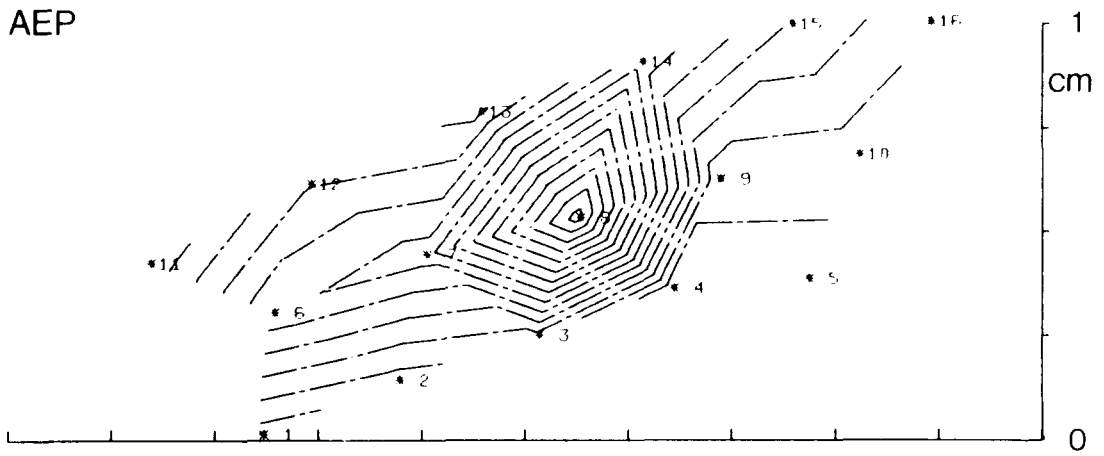
Comparisons of factor loading patterns were made within sessions by use of cross-correlation of the factor loading distributions. Averages of the correlations expressed by Z-transform are given in Table I for the 4 time periods and each of the 3 behavioral groups. The mean correlations were low, but they were significantly above zero, except in two instances. One was the set of factor loadings from the fourth time period in all 3 behavioral groups. The other was the set from the first (prestimulus) time period of the groups from the trials in which Chico appeared to be inattentive or responded outside the correct time frame.

The amplitude of a channel not only reflects the strength of the underlying activity but also the strength, size or depth of the cortical source as 'seen' by the electrode. For that reason we have attempted to make comparisons also after discarding the amplitude information. We achieved this by normalizing the variances in each channel to zero mean and unit standard deviation. When such a procedure was followed the cross-correlation values were lower (Table I, bottom). The only group that showed a significant positive Z-value was from the second time period trials after channel normalization ($Z = 0.599$) where the monkey had a correct response to the CS. The correlation ($Z = 0.141$) within the third epoch in the same trials might also have been significant. A significantly negative correlation ($Z = -0.376$, $P < 0.01$) was found between these two sets of factor loading patterns and not between any other sets.

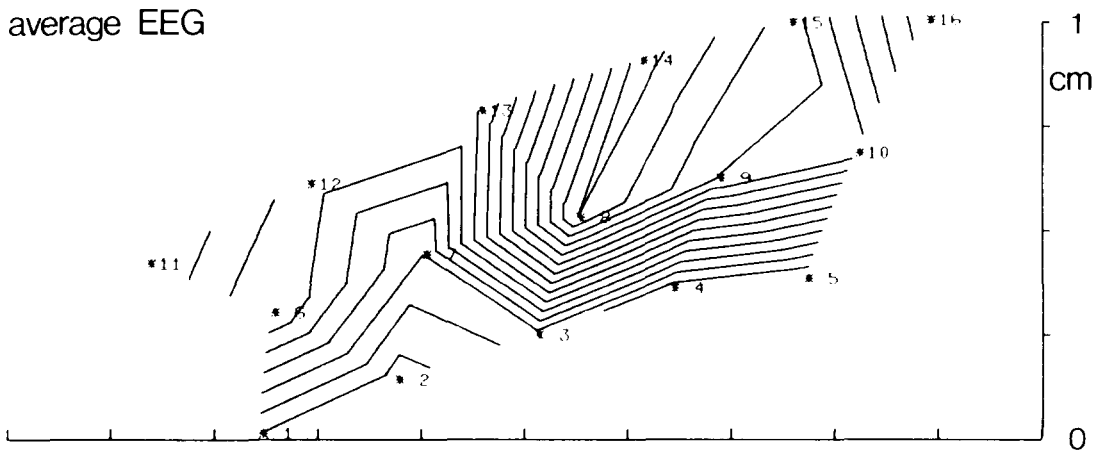
The cross-correlation test showed that after channel normalization* specific patterns might have existed for some of the epochs in some of the behav-

* When channel normalization is not applied, the Euclidian distance measure did not yield any significant results, since all spatial patterns were similar. We do not at present know the biophysical basis for the effect of this procedure and merely report that it holds both for olfactory bulbar and visual cortical EEGs.

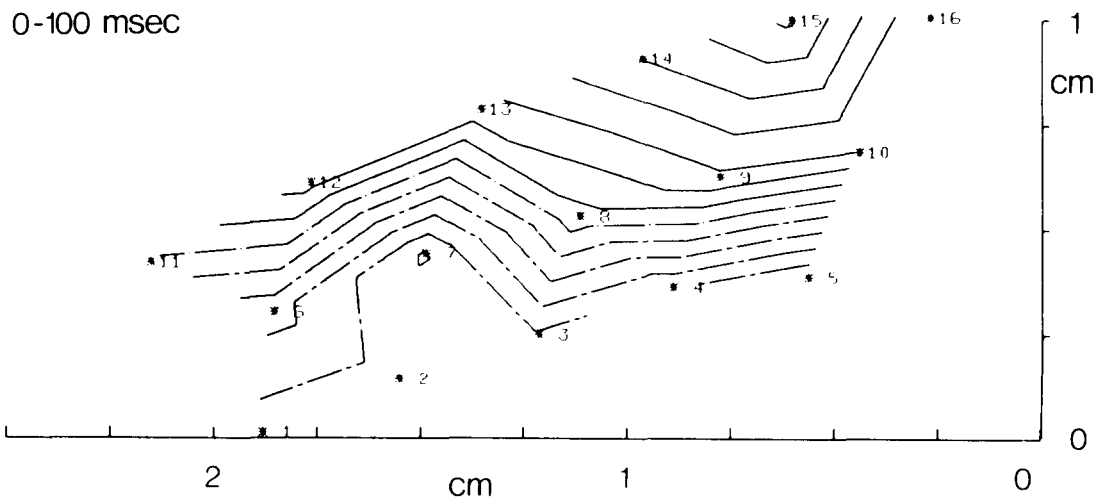
AEP



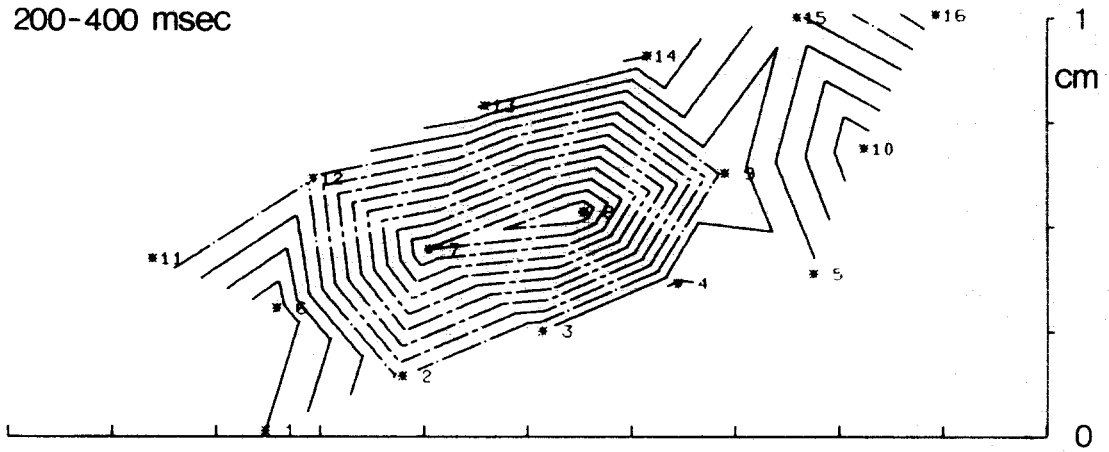
average EEG



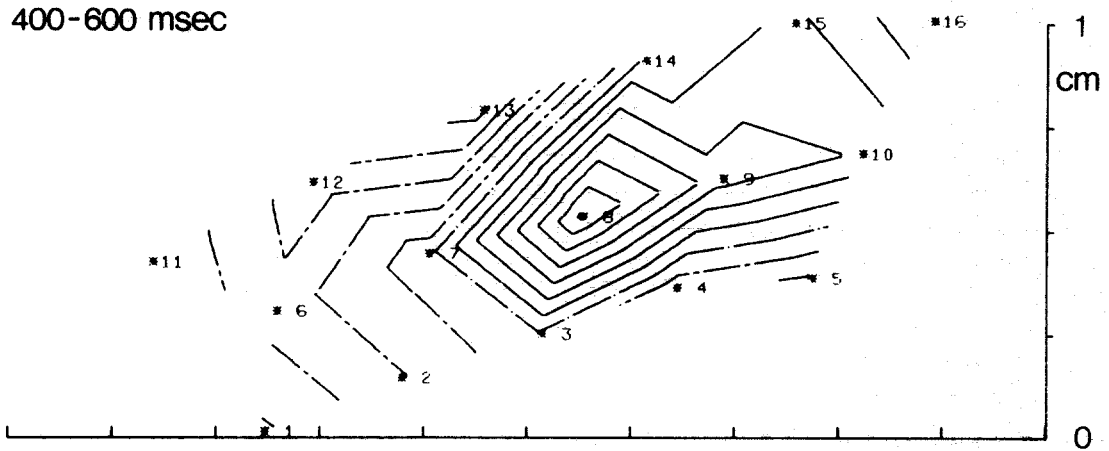
0-100 msec



200-400 msec



400-600 msec



600-800 msec

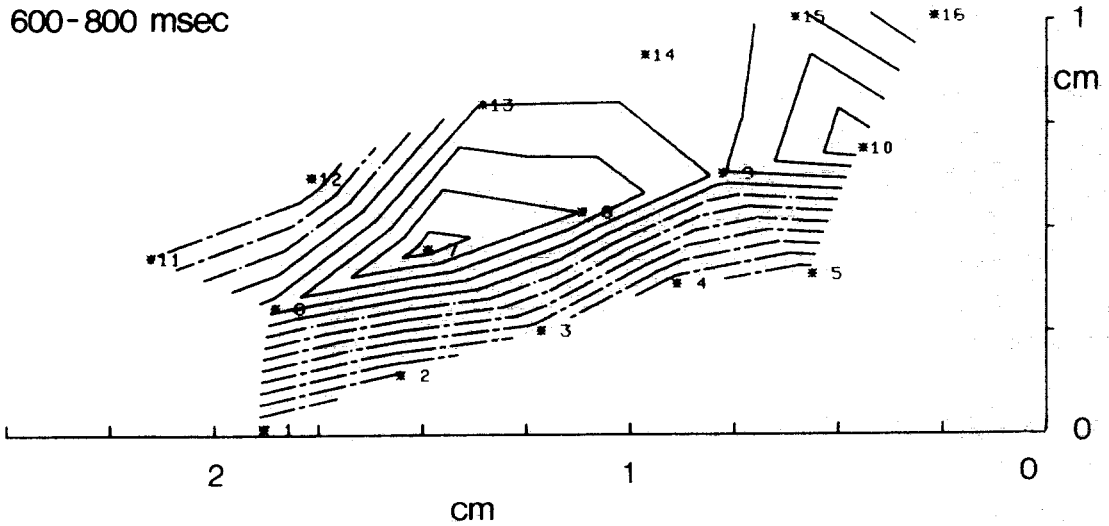


Fig. 4. Contour plots of the averages of factor loadings of the dominant component. Left: (above) averaged evoked potential; (middle) average of 64 representative 'bursts'; (below) average of 16 bursts from set 1 (0-100 ms) after channel normalization. Right: sets 2, 3 and 4 after channel normalization. The left edge of each frame is facing the midline; the upper edge is facing anteriorly. Channel 8 is nearest the foveal projection to the cortex. Each of the 4 sets is 'different' from all the others, but (except) for 2-3 and possibly 1-2) not 'significantly' due to the variability within sets.

TABLE I

Correlation values transformed to Fisher's Z-values from time periods and behavioral groups before and after normalization of the data by channel

Response	<i>n</i>	<i>S</i> ₁	<i>S</i> ₂	<i>S</i> ₃	<i>S</i> ₄	Between
<i>Group correlations (Fisher's Z)</i>						
Correct	20	0.342	0.475	0.410	0.244	0.370
Late	8	0.172	0.478	0.444	0.042	0.106
None	8	0.079	0.348	0.372	0.104	0.219
<i>After channel normalization</i>						
Correct	20	-0.076	0.599	0.141	-0.045	-0.116
Late	8	0.064	-0.073	-0.014	-0.098	-0.021
None	8	-0.035	0.006	-0.075	-0.070	-0.088

ioral states. Next we wanted to test whether these patterns were significantly different.

The Euclidean distance measure as described in the Materials and Methods section was used to test two hypotheses. The first was that the spatial pattern in the prestimulus epoch (0–100 ms) differed from the pattern in the second epoch just preceding the correct CR (200–400 ms), on the premiss that differing visual information was being processed in the two periods, flicker being present for the one and not for the other. The spatial patterns in the third (400–600 ms) and fourth (600–800 ms) epochs were used as a control set assuming that spatial patterns within the third and fourth epochs did not differ, there being no visual CS in this time period.

The results of the classification algorithm (Table II) showed that 67% of bursts were classified as correctly comparing the earlier two periods, whereas 52% were so classified comparing the later two periods. After correction from the control set values the percentage difference of the spatial patterns of bursts from epochs 1 and 2 was estimated to be between 15 and 31% (assuming additive and independent processes respectively). The hypothesis would be confirmed at $P = 0.01$.

The second was that the factor loading patterns differed between the second and third epochs, on the premise that Chico was looking at a significant CS in the second, and that he invariably looked down toward the reward spout as he pulled the reward lever.

TABLE II

Classification scores by a Euclidean distance measure

Upper set: hypothesis that patterns in periods 1 and 2 differed, but not those in 3 and 4. Difference values are given assuming additive processes (left) and assuming independent processes (right). Lower set: hypothesis that patterns in periods 2 and 3 differed, but not those in 1 and 4. A significance level of $P = 0.01$ for the %difference = 10% was established for the olfactory EEG from 64 electrodes. A significance level has not been established for the visual cortical EEG.

<i>Hypothesis 1</i>								
Response	<i>n</i>	<i>S</i> ₁	<i>S</i> ₂	%cor.	<i>S</i> ₃	<i>S</i> ₄	%cor.	%dif.
Correct	20	13	14	67	12	9	52	15–31
Late	8	3	5	50	7	1	50	0–0
None	8	4	6	62	5	4	56	6–14
<i>Hypothesis 2</i>								
		<i>S</i> ₂	<i>S</i> ₃		<i>S</i> ₁	<i>S</i> ₄		
Correct	20	16	20	90	6	6	30	60–86
Late	8	8	8	100	1	5	38	62–100
None	8	8	5	81	2	7	56	25–57

Using the factor loading patterns from bursts in the first and fourth epochs as controls, on the premise that any significant visual input was undefined or uncontrolled in these periods.

The classification algorithm sufficed to classify correctly 90% of bursts from the second and third epochs and 30% of bursts from the first and fourth epochs, resulting in estimates of the % difference between the spatial pattern of bursts from the second and third epochs of 60% and 76% assuming additive or independent probabilities respectively (Table II).

In conclusion, the results show that reproducible spatial patterns emerge from the EEGs after channel normalization, mainly in trials with correct CRs, and only in the periods corresponding with expected behaviorally significant visual input.

DISCUSSION

The theory for perception that was developed for the olfactory system holds that sensory information is brought to the bulb by action potentials on particular axons, and that it is rapidly integrated with past experience by a self-organizing mass action process involving the entire bulb^{3,5}. This process is manifested in oscillatory bursts that appear repeatedly in the EEG. It can be postulated that the entire visual cortex is organized similarly. If so, it can be predicted that the visual cortical EEG must have particular properties. First, the EEG must show a broad spectrum of chaotic background activity and repeated bursts in the high beta and gamma ranges¹. Second, there must be widespread spatial coherence, and the degree of coherence must fluctuate. Third, the spatial pattern of a component of the EEG that is widely distributed over the whole of the visual cortex must recur in multiple identifiable and reproducible forms. These forms must not simply be dependent on current sensory input, but also on the presence of particular types of stimuli that a subject has learned to discriminate, and on the presence of an appropriate motivational state, that is evidenced by goal-directed action following stimulus presentation.

These preliminary results from Chico conform to these requirements. It is observed that the visual cortical fast EEG resembles the olfactory EEG in several respects including its indifference to precise temporal frequencies; its tendency to recur in a charac-

teristic spatial pattern of amplitude (with its maximum near the foveal projection whereas the olfactory fast EEG has its largest amplitudes at or near possible olfactory 'foveas'^{3,7}); the high degree of variation between successive bursts around that characteristic pattern; and the enhanced efficacy of pattern retrieval by channel normalization, which effectively removes the characteristic pattern and the inequalities of the variances in the EEGs across channels. On the other hand the visual cortical EEG differs from the olfactory EEG in its lack of high amplitude bursts which for the olfactory EEG recur with respiration. The spectrum of long visual cortical EEG segments lacks a stable peak in the gamma range; instead it appears to conform to that of '1/f noise'. The differences in amplitudes of gamma activity may in part be attributable to the differences in anatomical structure between visual and olfactory cortices³⁻⁵; and the proper correlate for visual bursts might be found in eye movements rather than respiration. The presence of activity centered near 30 Hz rather than near 40 or 60 Hz may reflect species differences^{1,6}, differences between paleocortex and neocortex, or both.

Finally, present evidence for spatial pattern differences relating to CS and CR by itself is unconvincing. It will be required to use multiple CSs and show that spatial patterns emerge that are stable, that they depend on the CS given, and that they change while the animal is being trained.

Requirements for further study include use of a larger number of channels for simultaneous recording, such as 32 to 64 or more in a larger array window, and a greater number of trials and bursts within trials. Use of digital adaptive filters³ may be preferable to PCA for decomposing EEGs and extracting spatio-temporal patterns. Also records should be included of time markers for the CS, CR, US and UR; the EMGs from several locations in order to evaluate the extent of contamination on the subdural recordings; and of eye movements, especially of saccades for possible use as time markers for the segmentation of EEGs prior to decomposition.

The requirements for large numbers of electrodes covering a large array window and for extensive discriminative conditioning are not easily met in using animals. However, the theory requires that spatially coherent activity exist over extensive regions of cortex. The spatial extent of coherence found in records

from Chico indicate that spatial patterns of fast EEG activity should be accessible from scalp electrodes, with an acceptable degree of spatial smoothing by the skull and soft tissues intervening. A non-invasive approach with scalp electrodes in humans might be preferable to animal studies for some areas of cortex, although not for the visual, owing to its high degree of infolding within the interhemispheric fissure in humans.

REFERENCES

- 1 Bressler, S.L. and Freeman, W.J., Frequency analysis of olfactory system EEG in cat, rabbit and rat, *Electroencephalogr. Clin. Neurophysiol.*, 5 (1980) 19–24.
- 2 Dagnelie, G., *Pattern and Motion Processing in Primate Visual Cortex. A Study in Visually Evoked Potentials*, Thesis, University of Amsterdam, 1986, 326 pp.
- 3 Freeman, W.J., Techniques used in the search for the physiological basis of the EEG. In A. Gevins and A. Remond (Eds.), *Handbook of Electroencephalography and Clinical Neurophysiology, Vol. 3A*. Elsevier, Amsterdam, 1987, in press.
- 4 Freeman, W.J., Repetitive seizure spikes in olfactory bulb and cortex caused by runaway inhibition after exhaustion of excitation, *Brain Res. Rev.*, 11 (1986) 259–284.
- 5 Freeman, W.J. and Skarda, C.A., Spatial EEG patterns, non-linear dynamics and perception: the neo-Sherringtonian view, *Brain Res. Rev.*, 10 (1985) 147–175.
- 6 Lopes da Silva, F.H., Van Rotterdam, A., Storm van Leeuwen, W. and Tielen, A.M., Dynamic characteristics of visual evoked potentials in the dog. II. Beta frequency selectivity in evoked potentials and background activity, *Electroencephalogr. Clin. Neurophysiol.*, 29 (1970) 260–268.
- 7 Maier, J., Dagnelie, G., Van Dijk, B.W. and Spekreijse, H., Principal components analysis for source localization of VEPs in man, *Vision Res.*, 27/2 (1987) 165–177.
- 8 Meisami, E. and Emamian, S., Cytoarchitectural diversity in the main olfactory bulb: are these olfactory foveal?, *Am. Chemosens. Soc.*, VIII (1985) Abstr. 130.
- 9 Schuster, H.G., *Deterministic Chaos*, Springer, Berlin, 1984.

ACKNOWLEDGEMENTS

Supported by Grant MH06686 from the National Institute of Mental Health. Experiments were carried out at The Netherlands Ophthalmic Research Institute. The generous support and encouragement of Prof. H. Spekreijse, and prior work by Dr. G. Dagnelie, are gratefully acknowledged.